One- and Two-Photon Spectra of Platinum Acetylide Chromophores: A TDDFT Study

Kiet A. Nguyen,[†,‡] Paul N. Day,[†,‡] and Ruth Pachter*

Materials and Manufacturing Directorate, Air Force Research Laboratory, Wright-Patterson Air Force Base, Ohio 45433

Received: June 24, 2009; Revised Manuscript Received: September 28, 2009

We report one- (OPA) and two-photon absorption (TPA) excitation energies and cross-sections for a series of platinum acetylides using time-dependent density functional theory. Because of the facile rotations of the trimethylphosphinyl and phenylene groups, we apply a Boltzmann-weighted average over thermally accessible conformations to obtain the final spectra, resulting in better agreement with experimental observations. We examine various basis sets and functionals to evaluate their performance in the gas-phase and in solution. Effects of donor and acceptor groups on the OPA and TPA resonances and intensities are also discussed.

1. Introduction

Platinum acetylides[1] are of interest because of their applications in light-emitting diodes.[2,3] Trialkylphosphine platinum acetylides with one platinum (**1**−**2**) center (Figure 1), in particular, have been extensively studied because of their strong nonlinear optical reponses,[4−8] which were attributed to two-photon absorption (TPA)[6,8,9] and excited state one-photon absorption (OPA).[10−13]

Theoretically, TDDFT[14−17] OPA and TDHF TPA spectra of various platinum acetylide complexes were first reported by Norman et al.[18] For $Pt(PH_3)_2(C{\equiv}C-Ph)_2$ and $Pt(PH_3)_2(C{\equiv}C-Ph-C{\equiv}C-Ph)_2$, the C_{2v} conformer was considered. The ground state and T_1 properties of tributylphosphine complexes $Pt(PH_3)_2(C{\equiv}C-Ph)_2$[19,20] and $Pt(PH_3)_2(C{\equiv}C-Ph-C{\equiv}C-H)_2$[19] have been reported using the B3LYP functional. Cooper et al. reported DFT studies for trimethylphosphine analogs of **2**[21] and for a series of symmetric and asymmetric acetylides[7] using PW91 and B3LYP functionals, respectively. Recently, Minaev et al.[22] reported a detailed TDDFT/DFT study of ground S_0-S_n and S_0-T_n spectra and the T_1 excited state structures and energetics for a number of conformers of $Pt(PH_3)_2(C{\equiv}C-Ph)_2$ and $Pt(PH_3)_2(C{\equiv}C-Ph-C{\equiv}C-Ph)_2$ using the B3LYP functional. For $Pt(PH_3)_2(C{\equiv}C-Ph)_2$, they found that a nonplanar structure with twisted phenyl rings provides better agreement with the X-ray crystallographic structure of singlet−singlet absorption spectra of trialkylated phosphine derivatives.

The present work focuses on trialkylphosphine platinum acetylides with one platinum center and different C≡C−L ligands with different donor or acceptor L groups (summarized in Figure 1) that were reported to exhibit large TPA cross-sections.[8] The ethynyl−benzothiazolylfluorene ligands in **3** act as electron acceptors, whereas the ethynyl−diphenylaminolfluorene ligands in **4** act as electron donors. The nonsymmetric donor−acceptor (**5**) has not been previously considered. Effects of the donor and acceptor are gauged by using the phenylethynyls −C≡C−Ph (**1**) and −C≡C−Ph−C≡C−Ph (**2**) as references (Figure 1). Previous TDDFT studies reported first excitation energies and oscillator strengths for some conformers of platinum acetylides.[23]

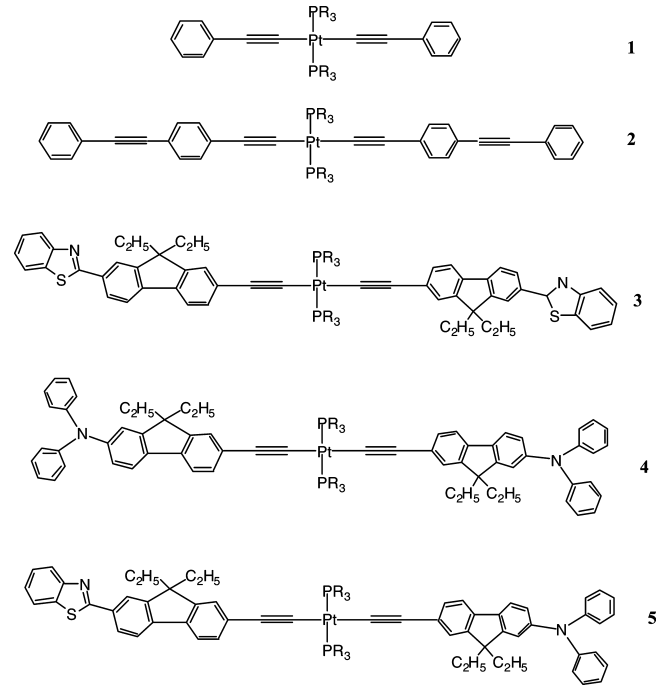

Figure 1. Structures of platinum complexes.

However, TPA calculations were carried out using the INDO/S sum-overstate method with modified values for β_{sp} and β_d. In this work, we rigorously investigate both the OPA and TPA spectra for the series of platinum acetylides in the gas phase and in solvent using linear and quadratic TDDFT response methods. The results provided insight into effects of alkylation, whereas careful comparison with experimental spectra was obtained by Boltzmann weighting averaged over thermally accessible conformations to obtain the final spectra, which was found to be important to account for the observed spectra of some chromophores. TPA predictions were in good agreement with experiment using improved functionals.

2. Computational Methods

The computation of excitation energies and cross-sections was preceded by the determination of equilibrium geometries; then, single-point excited state calculations were carried out to obtain

* Corresponding author.
† Current address: UES, Inc.
‡ Current address: General Dynamics Information Technology, Inc.

10.1021/jp905921v CCC: $40.75
Published on Web 11/17/2009

the vertical excitation energies, transition dipole moments, and oscillator strengths. Structural predictions were carried out using the Kohn−Sham (KS)[24] density functional theory with the 6-311G(d,p)[25] basis set and the B3LYP hybrid functional.[26−28] These structures were verified to be minima on the potential energy surface by harmonic frequency calculations using the Gaussian 03 program.[29] For selected cases, DFT/TDDFT calculations were carried out using the 6-311G(d,p), 6-311++G(d,p), and aug-cc-pVTZ basis sets with the B3LYP, PBE0, and the hybrid functional of Yanai et al. (CAMB3LYP),[30] as implemented in Dalton.[31]

To account for the solvent effects, TDDFT calculations were carried out with the nonequilibrium polarizable continuum model[32,33] (PCM) using a locally modified version of the Dalton program,[31] in which the same united atom (UA0) cavity definition as that implemented in the Gaussian 03 program[29] was used. The PCM solute cavities determination was carried out using the interlocking-sphere model and empirical solvent radii. Atomic UFF van der Waals radii (R_i^{UFF}) were used with the following added adjustment factors (γ_i^{UA0}) to build the UA0 cavity

$$R_i^{UA0} = R_i^{UFF} + n_i\gamma_i^{UA0} \quad (1)$$

where n_i is the number of bonded atoms. γ_i^{UA0} is taken to be 0 for the first period elements, 0.1 Å for N and O, and 0.2 Å for other elements.

For the OPA spectra, the extinction coefficients are computed as

$$\varepsilon(\tilde{\nu}) = \frac{2\sqrt{\ln 2}}{4.32\times10^{-9}\sqrt{\pi}}\sum_i g_i(Q_i)\sum_f \frac{f_{0f}(Q_i)}{\tilde{\nu}_f^{FWHM}} \times \exp\left[\frac{-4\ln 2}{(\tilde{\nu}_f^{FWHM})^2}(\tilde{\nu} - \tilde{\nu}_{0f}(Q_i))^2\right] \quad (2)$$

where $g(Q_i)$, $f_{0f}(Q_i)$, and $\tilde{\nu}_{0f}(Q_i)$ are the Boltzmann factor, oscillator strength, and transition frequency for a given Q_i geometry, respectively. Similarly, by relating the absorption rate[34,35] to the TPA transition probability, which was first derived by Goppert-Mayer using second-order perturbation theory,[36] the TPA cross-sections (δ) can be written as

$$\delta(2E_\lambda) = \frac{16\pi^4}{c^2h}\left(\frac{\ln 2}{\pi}\right)^{1/2}E_\lambda^2\sum_i g_i(Q_i)\sum_f \frac{|S_{f0}(Q_i)|^2}{E_f^{FWHM}} \times \exp\left\{\frac{-4\ln 2}{(E_f^{FWHM})^2}[2E_\lambda(Q_i) - E_f(Q_i)]^2\right\} \quad (3)$$

where c is the speed of light, h is the Planck's constant, E_λ represents the photon energies, and the normalized line shape function is taken as a Gaussian. The two-photon matrix elements $S_{f0}(Q_i)$ were obtained from the single-residue of the quadratic response (SRQR) function of the electric dipole operator[37] within the framework of TDDFT[38] using the Dalton program.[31]

3. Results and Discussion

A. Chromophores 1 and 2. *Effects of Alkyl Groups.* Chromophores **1** and **2** were synthesized with trialkylphoshine axial ligands, including trimethylphosphine ligands.[1,4−8] The

TABLE 1: TD-mCAMB3LYP/HW-6-31G* Relative Ground (kilocalories per mole), OPA Excitation Energy (*E*, electronvolts), and Oscillator Strength (*f*) for Methyl Analogs of 1[a]

a			b			c			d			e			f			g			h		
state	*E*	*f*	state	*E*	*f*	state	*E*	*f*	state	*E*	*f*	state	*E*	*f*	state	*E*	*f*	state	*E*	*f*	state	*E*	*f*
1^1A_g	0.00		1^1A_1	0.1		1^1A	0.3		1^1A_g	0.7		1^1A_1	0.8		$1^1A'$	0.3		1^1A_1	0.6		1^1A_1	0.4	
1^1A_u	4.11	0.00	1^1A_2	4.08		1^1B	3.95	0.56	1^1B_u	3.70	0.85	2^1A_1	3.70	0.85	$2^1A'$	3.95	0.60	2^1A_1	3.92	0.60	2^1A_1	3.98	0.60
1^1B_u	4.35	0.08	2^1A_1	4.35	0.08	2^1A	4.07	0.00	1^1A_u	4.10	0.00	1^1A_2	4.07		$1^1A''$	4.05	0.00	1^1A_2	4.07		1^1A_2	3.99	
2^1A_u	4.51	0.00	2^1A_2	4.50		2^1B	4.46	0.00	1^1B_g	4.35		1^1B_1	4.34	0.00	$2^1A''$	4.45	0.00	1^1B_1	4.41	0.00	1^1B_1	4.46	0.00
1^1B_g	4.53		3^1A_2	4.56		3^1B	4.50	0.13	2^1B_g	4.51		3^1A_1	4.61	0.00	$3^1A''$	4.50	0.00	2^1A_2	4.47		2^1A_2	4.55	
2^1B_g	4.58		1^1B_2	4.57	0.00	3^1A	4.59	0.00	2^1A_g	4.60		2^1A_2	4.53		$4^1A''$	4.52	0.00	3^1A_2	4.50		3^1A_2	4.56	
3^1B_g	4.67		1^1B_1	4.65	0.00	4^1A	4.78	0.00	2^1B_u	4.82	0.01	1^1B_2	4.82	0.01	$3^1A'$	4.78	0.63	3^1A_1	4.80	0.77	1^1B_2	4.73	0.01
2^1A_g	4.67		4^1A_2	4.67		4^1B	4.88	0.50	3^1A_g	4.82		2^1B_2	4.82	0.00	$4^1A'$	4.79	0.15	1^1B_2	4.81	0.00	3^1A_1	4.77	0.79
2^1B_u	4.71	1.55	3^1A_1	4.70	1.53	5^1A	4.89	0.01	4^1A_g	4.91		5^1A_1	4.90	0.01	$5^1A'$	4.84	0.00	1^1B_2	4.84	0.00	2^1B_2	4.85	0.00
3^1A_g	4.92		1^1B_2	4.90	0.01	6^1A	5.01	0.00	5^1A_g	4.99		3^1B_2	4.96	0.00	$5^1A''$	4.93	0.01	2^1B_1	4.95	0.00	2^1B_1	4.91	0.01
3^1A_u	4.92	0.01	4^1A_1	4.92	0.00	5^1B	5.04	0.34	2^1A_u	5.03	0.05	2^1B_1	5.04	0.05	$6^1A'$	5.06	0.00	4^1A_1	5.07	0.00	4^1A_1	5.03	0.00
4^1A_g	5.13		2^1B_2	4.94	0.00				3^1B_u	5.07	0.38	6^1A_1	5.08	0.36	$6^1A''$	5.14	0.05	3^1B_1	5.15	0.05	3^1B_1	5.15	0.05
4^1A_u	5.29	0.05	5^1A_1	5.13	0.00				3^1B_g	5.36		7^1A_1	5.15	0.01	$7^1A'$	5.16	0.00	5^1A_1	5.15	0.00	5^1A_1	5.15	0.00
3^1B_u	5.34	0.07	3^1B_2	5.29	0.05				3^1A_u	5.38	0.00	3^1A_2	5.30		$8^1A'$	5.23	0.12	4^1A_2	5.33		6^1A_1	5.21	0.11

[a] Experimental absorption maxima: 3.83 eV, ε = 24 700 ± 500 M^{-1} cm^{-1}, f = 0.38 in benzene.[12] 3.80 eV in CH_3CN, 3.81 eV in 1:1 benzene/CH_3CN.[41]

TABLE 2: TD-mCAM3LYP/HW-6-31G* Relative Ground (kilocalories per mole), OPA Excitation Energy (*E*, electronvolts), and Oscillator Strength (*f*) for Methyl Analogs of 2[a]

a			b			c			d			e			f			g			h		
state	*E*	*f*	state	*E*	*f*	state	*E*	*f*	state	*E*	*f*	state	*E*	*f*	state	*E*	*f*	state	*E*	*f*	state	*E*	*f*
1^1A_g	0.0		1^1A_1	0.1		1^1A	0.0		1^1A_g	0.7		1^1A_1	0.9		$1^1A'$	0.4		1^1A_1	0.6		1^1A_1	0.4	
1^1B_u	3.65	3.64	2^1A_1	3.65	3.61	1^1B	3.64	3.72	1^1B_u	3.24	2.83	2^1A_1	3.24	2.82	$2^1A'$	3.49	2.97	2^1A_1	3.47	2.85	2^1A_1	3.50	3.09
2^1A_g	3.86		3^1A_1	3.86	0.01	2^1A	3.82	0.00	2^1A_g	3.78		3^1A_1	3.78	0.00	$3^1A'$	3.80	0.68	3^1A_1	3.81	0.79	1^1A_2	3.77	
1^1A_u	4.03		1^1A_2	4.02		3^1A	4.00	0.00	1^1A_u	3.90	0.00	1^1A_2	3.88		$1^1A''$	3.83	0.00	1^1A_2	3.85		3^1A_1	3.79	0.56
2^1A_u	4.06	0.00	2^1A_2	4.03		2^1B	4.03	0.01	3^1A_g	4.08		4^1A_1	4.07	0.07	$2^1A''$	3.92	0.00	2^1A_2	3.86		2^1A_2	3.97	
1^1B_g	4.14	0.00	3^1A_2	4.14		4^1A	4.11	0.00	1^1B_g	4.21		2^1A_2	4.23		$3^1A''$	4.24	0.00	3^1A_2	4.23		3^1A_2	4.28	
2^1B_u	4.31	0.30	4^1A_1	4.21	0.17	4^1B	4.30	0.03	2^1B_u	4.25	0.76	5^1A_1	4.25	0.70	$4^1A'$	4.30	0.07	4^1A_1	4.29	0.08	4^1A_1	4.31	0.07
3^1A_g	4.33		5^1A_1	4.37	0.17	5^1A	4.39	0.00	2^1B_g	4.34		1^1B_1	4.32	0.00	$4^1A''$	4.44	0.00	1^1B_1	4.41	0.00	1^1B_1	4.46	0.00
2^1B_g	4.42		4^1A_2	4.45		5^1B	4.44	0.00	3^1B_u	4.48	0.09	6^1A_1	4.47	0.10	$5^1A'$	4.58	0.00	1^1B_2	4.58	0.00	4^1A_2	4.48	
3^1B_u	4.45	0.02	6^1A_1	4.50	0.00	6^1B	4.57	0.16	3^1A_g	4.57		1^1B_2	4.57	0.00	$5^1A''$	4.59	0.00	5^1A_1	4.61	0.03	1^1B_2	4.58	0.00
3^1A_u	4.62	0.00	1^1B_1	4.62	0.00	6^1A	4.65	0.00	3^1B_g	4.84		2^1B_2	4.57	0.00	$6^1A'$	4.61	0.03	4^1A_2	4.62		5^1A_1	4.59	0.03

[a] Experimental absorption maxima: 3.49 eV ε = 89 000 ± 1200 $M^{-1}cm^{-1}$, f = 1.80 in benzene;[12] 3.54 eV in 1:1 benzene/CH_3CN.[41] INDO/s: 3.28 eV, f = 2.67; TD-B3LYP: 3.41 eV, f = 2.67.[23]

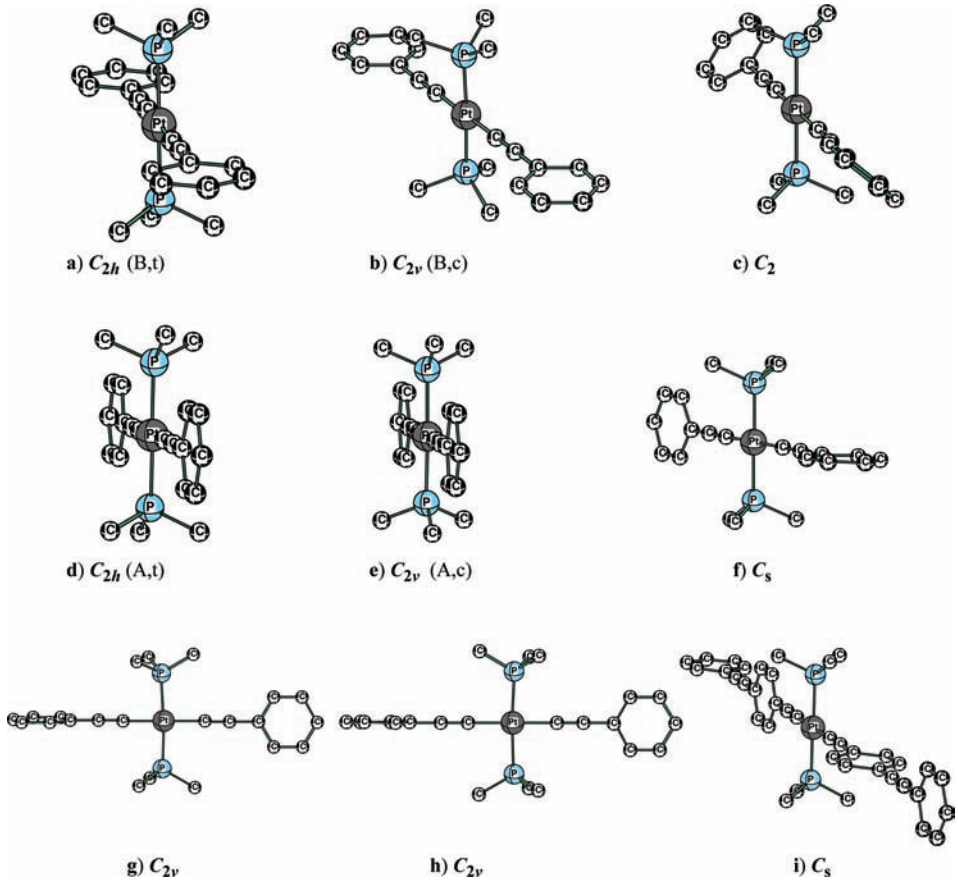

Figure 2. Structural conformers of **1** (**a**−**g**). (**a**) All atoms in the phenyl rings. Except for the **i** conformer, conformers **a**−**h** of **2** have two parallel aligned ethynylphenyl groups.

unsubstituted analogs of **1** and **2** with phosphine ligands were not experimentally reported but were examined theoretically.[18,22] Effects of alkyl groups were also studied for $Pt(PH_3)_2(C{\equiv}CH)_2$.[22] In this work, we extended the chain length of the trialkylphosphine groups from methyl to *n*-butyl to examine their influence on the ground state OPA spectrum of **1**. The unsubstituted analog of **1** with phosphine ligands was also examined. Starting with the trimethyphosphine analog of **1**, the anti straight-chain extension of all three alkyl group leads to structures that are higher in energy than the alternate antiequatorial-anti forms. The anti straight-butyl derivative of **1** was also previously considered.[19,20] For the **a** conformer with C_{2h} symmetry, we found that substitution of phosphine for tributylphosphine shifts the S_0-S_1 energy by ~0.5 eV. (See the Supporting Information, Table 1S.) Note that alkylation switches the symmetry of S_1 from A_g to A_u. In contrast, the increase in chain length from methyl to *n*-butyl has a very small effect on the excitation energies and oscillator strengths. The largest shift of 0.08 eV was obtained for S_0-S_1. Similar results were obtained in solvent (benzene) PCM calculations (Supporting Information, Table 2S). Because of the small effects of the alkyl chains observed for **1**, trimethylphosphine ligands are selected to reduce the computation cost for the calculation of **2**, **3**, **4**, and **5**. Chromophores **2**, **3**, and **4** with trimethylphosphine ligands have been previously considered using TDDFT and INDO/s.[23] However, only one conformer was considered for **2**. For **3** and **4**, spectral results for two conformers (centrosymetric C_i and C_1 structures) were reported. The TDDFT results reported for the first excited state of these conformers are almost identical to our computed B3LYP values (Supporting Information, Tables 4S−6S).

Effects of Basis Sets and Functionals. We examined basis set effects with a trimethylphosphine derivative of **1** (Supporting Information, Table 3S). At the B3LYP/LANL2DZ-6-31G(d) geometry, the inclusion of *f*-polarization functions has negligible (within 0.02 eV) effects on the excitation energy and oscillator strength. The excitation energy and oscillator strength obtained at the optimized B3LYP/SDD-aug-cc-pVTZ geometries with and without the inclusion of *f*-polarization functions also have negligible differences (within 0.02 eV) for the first six excited states. The next two excited states blue-shift by 0.04 and 0.05 eV, respectively, with the inclusion of *f*-polarization functions.

Three functionals, B3LYP, CAMB3LYP, and mCAMB3LYP, were applied with the LANL2DZ (for Pt) and 6-31G(d) basis sets. As reported for other donor−acceptor chromophores,[39,40] B3LYP and CAMB3LYP were found to underestimate and overestimate excitation energies, respectively. The oscillator strengths were overestimated by all functionals. The trends appear to correlate with the amount of HF exchange, B3LYP < mCAMB3LYP < CAMB3LYP, but are reversed for TPA intensity. Qualitative spectral assignments are not affected by functionals used. The relative S_0 energies are not significantly affected by the functionals used. Therefore, the mCAMB3LYP results are used for discussion for all chromophores.

One-Photon Absorption Spectra. The excitation energies and oscillator strengths for different conformers of **1** and **2** are listed in Tables 1 and 2. Their ground-state energies relative to the lowest-energy conformer are also included. The geometries of different conformations of **1** and **2** are alphabetically (**a**−**i**) labeled in Figure 2. Except for the **i** form of **2**, relative energies of these isomers are all within 1 kcal/mol. The lowest (**a** form) energy isomer is found to have staggered trimethylphosphines and phenylene planes that are orthogonal to the P−Pt−P axis. Rotation of the trimethylphosphinyl groups is facile, leading to the **b** conformer that lies only 0.1 kcal/mol higher than the

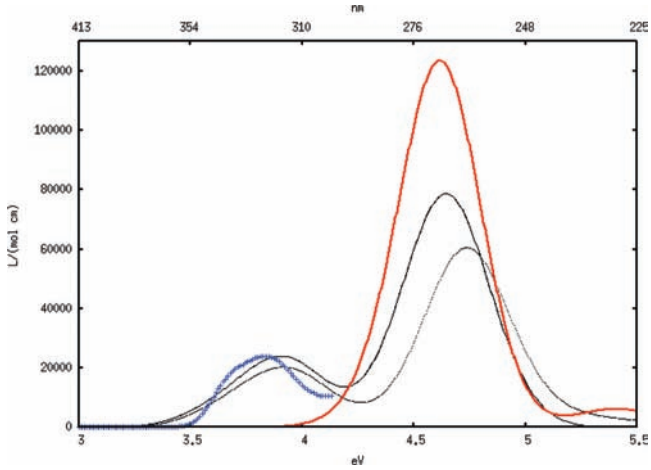

Figure 3. OPA spectra for **1**. Experimental spectrum obtained in benzene at room temperature (+). Computed PCM spectra obtained using fwhm of 0.42 for the lowest (**a**) conformer (bold, red) and Boltzmann conformational (**a**−**h**) averaged at 298.15 K (solid). Computed gas-phase spectra obtained using fwhm of 0.42 with Boltzmann conformational (**a**−**h**) averaged at 298.15 K (dots).

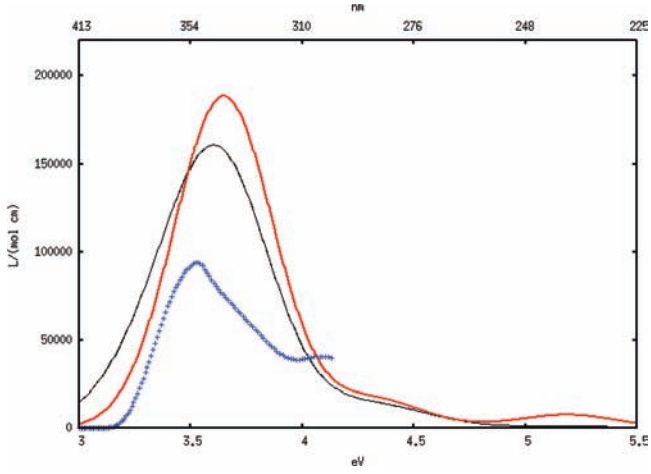

Figure 4. OPA spectra for **2**. Experimental spectrum obtained in benzene at room temperature (+). Computed spectra obtained using fwhm of 0.52 for the lowest (**a**) conformer (bold, red) and Boltzmann conformational (**a**−**h**) averaged at 298.15 K (solid).

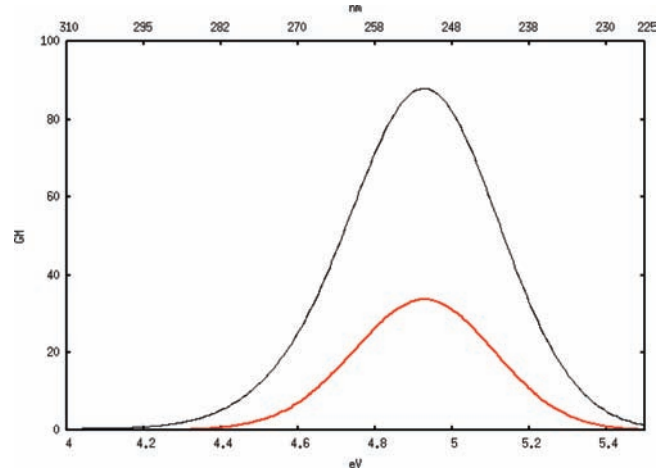

Figure 5. Calculated TPA spectra for **1** using fwhm of 0.42 for the lowest (**a**) conformer (bold, red) and Boltzmann conformational (**a**−**h**) averaged at 298.15 K (solid).

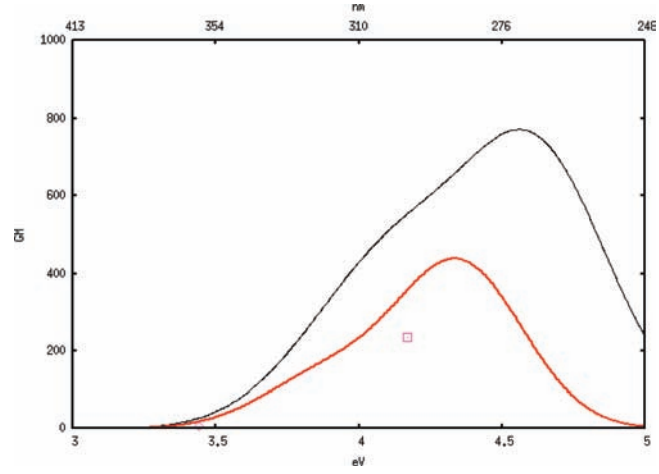

Figure 6. Calculated TPA spectra for **2** using fwhm of 0.42 for the lowest (**a**) conformer (bold, red) and Boltzmann conformational (**a**−**h**) averaged at 298.15 K (solid). Experimental values for *n*-butyl analog measured in CH_2Cl_2 using 27 ps laser pulses (square) of Mackay et al.[9] and in THF using 180 fs laser pulses (diamond) of Glimsdal et al.[43]

lowest energy C_{2h} **a** conformer. Geometry optimization starting from a twisted-phenylene **b** form with C_1 symmetry converges to planar C_{2v} **b** conformer. Symmetric (**c**) and nonsymmetric (**f**, **g**, **h**) twisting of the phenylene rings also increases the energy. Interestingly, geometry optimization starting from a modified (**c**) form that has two different Pt−C bonds leads to the lowest-energy C_{2h} **a** conformer. The rotation and twisting of the phenylene rings increase the energy (0.2 to 0.7 kcal/mol). In contrast, the effects of phenylene rotations on the excited states are quite large for **1**, as previously noted for the phosphine derivative.[22] For **1**, the lowest conformer fails to account for the observed S_0-S_n OPA spectrum. The symmetric and nonsymmetric **c** conformers with twisted phenylene rings provide better agreement with experiment. Because the observed spectrum is averaged over thermally accessible conformations, we apply a Boltzmann weighted average over all conformations at room temperature (298.15° K) to obtain the final spectra for comparison with experiment. The results are shown in Figure 3. The averaged spectrum in the gas phase has the first maximum

TABLE 3: TD-mCAMB3LYP/HW-6-31G* TPA Excitation Energy (*E*, in electronvolts) and Cross-Section ($\delta \geq 1$, in GM) Using Gaussian Line Shape and Experimental OPA FWHM of 0.42 eV for 1[a]

a			**b**			**c**			**d**			**e**			**f**			**g**			**h**		
state	*E*	δ	state	*E*	δ	state	*E*	δ	state	*E*	δ	state	*E*	δ	state	*E*	δ	state	*E*	δ	state	*E*	δ
3^1A_g	4.67	1	1^1B_1	4.65	1	2^1A	4.35	1	3^1A_g	4.60	46	2^1A_1	3.70	1	$3^1A'$	4.78	6	3^1A_1	4.80	8	1^1B_2	4.73	1
4^1A_g	4.92	33	3^1A_1	4.92	35	3^1A	4.88	8	3^1A_g	4.82	2	3^1A_1	4.61	42	$4^1A'$	4.79	2	1^1B_2	4.81	1	3^1A_1	4.77	8
						4^1A	5.12	1	4^1A_g	4.91	473	2^1B_2	4.82	1	$5^1A'$	4.84	1	2^1B_2	4.84	1	1^1B_2	4.85	1
						4^1A	5.13	1	5^1A_g	4.99	2	4^1A_1	4.90	460	6A′	5.06	31	4^1A_1	5.07	34	4^1A_1	5.03	28
												5^1A_1	5.08	16				5^1A_1	5.15	6	5^1A_1	5.15	1
												6^1A_1	5.15	26									

[a] Boltzmann averaged maxima at 298.15 K: 4.93 eV (88 GM).

TABLE 4: TD-mCAMB3LYP/HW-6-31G* TPA Excitation Energy (*E*, in electronvolts) and Cross-Section ($\delta \geq 1$, in GM) Using Gaussian Line Shape and Experimental OPA FWHM of 0.52 eV for 2[a]

a			b			c			d			e			f			g			h		
state	*E*	δ	state	*E*	δ	state	*E*	δ	state	*E*	δ	state	*E*	δ	state	*E*	δ	state	*E*	δ	state	*E*	δ
2^1A_g	3.86	133	3^1A_1	3.86	137	2^1A	3.82	104	2^1A_g	3.78	188	3^1A_1	3.24	3	$2^1A'$	3.49	8	2^1A_1	3.47	7	2^1A_1	3.50	8
3^1A_g	4.08	422	4^1A_1	4.21	171	3^1A	4.00	1	3^1A_g	4.08	2508	4^1A_1	3.78	204	$3^1A'$	4.30	79	3^1A_1	3.81	62	3^1A_1	3.79	95
			5^1A_1	4.37	119	4^1A	4.11	17				5^1A_1	4.07	2340	$4^1A'$	4.61	1734	4^1A_1	4.29	141	4^1A_1	4.31	32
			6^1A_1	4.50	142	5^1A	4.39	389				6^1A_1	4.25	56				5^1A_1	4.61	1760	5^1A_1	4.59	1685
			1^1B_2	4.62	3	6^1A	4.65	3				7^1A_1	4.47	123				2^1B_2	4.81	2	2^1B_2	4.70	2
																		6^1A_1	4.83	616	3^1B_1	4.82	2
																		3^1B_1	4.85	2	3^1B_2	4.83	2
																					5^1A_1	4.86	723

[a] TPA maximum 4.17 eV of and cross-section of 235 GM measured in benzene for *n*-butyl analog using 27 ps laser pulses.[42] Single-wavelength (720 nm, 3.44 eV) cross-section of 7 GM measured in THF using 180 fs laser pulses.[6] Single-wavelength (740 nm, 3.35 eV) cross-section of 7 GM measured in THF using 180 fs laser pulses.[43] Boltzmann averaged maxima at 298.15 K: 4.57 eV (771 GM). INDO/s: 3.47 eV (138 GM), 4.15 eV (192 GM).[23]

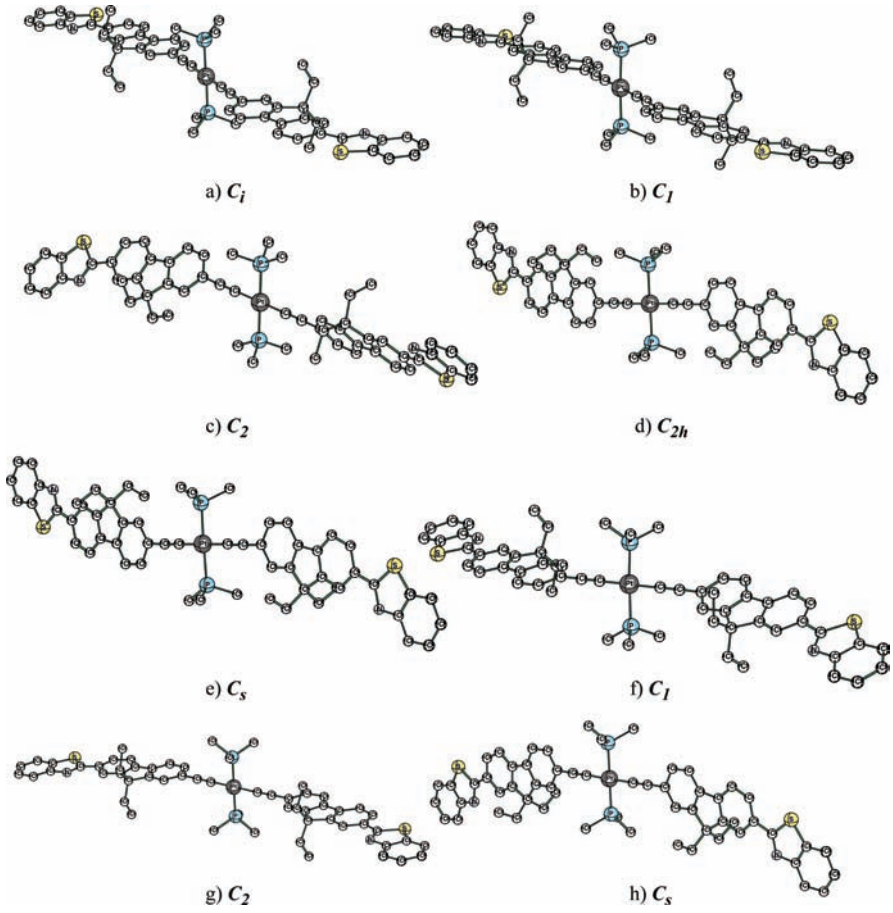

Figure 7. Structural conformers of **3**.

at 3.92 eV with the extinction coefficient (ε) of 20 300 M^{-1} cm^{-1}. In benzene, this band shifts slightly to red (3.91 eV) with increasing intensity (ε = 24 100 M^{-1} cm^{-1}), as predicted by PCM calculations. The computed results are in good agreement with the observed maxima, 3.83 eV, and intensity of 24 700 ± 500 M^{-1} cm^{-1} in benzene;[12] 3.80 eV in CH_3CN; and 3.81 eV in 1:1 benzene/CH_3CN.[41] The S_0-S_1 transition has a small amount of metal-to-ligand CT character because the HOMO of all **1** conformers has some metal contributions, as previously shown for the triphosphine[22] and tributylphosphine[19,20] derivatives.

For **2**, all conformers are predicted to have intense S_0-S_1 transitions (Table 2) with a Boltzmann weighted averaged maximum of 3.61 eV (Figure 4), a red shift of 0.31 eV compared with **1**. The computed peak of 3.61 eV is slightly lower than the first excitation energy of the lowest-energy conformer (3.65 eV). These computed values compare well with the observed maxima and shifts: 3.49 eV and a red shift of 0.34 eV in benzene[12] and 3.54 eV and a red shift of 0.27 eV in 1:1 benzene to CH_3CN.[41] However, the predicted peak intensity of 160 000 M^{-1} cm^{-1} is 80% larger than the observed value (89 000 ± 1200 M^{-1} cm^{-1}) in benzene.[12] The corresponding predicted peak energy (3.41 eV) and intensity (142 000 M^{-1} cm^{-1}) obtained from B3LYP are slightly smaller. The S_0-S_1B3LYP excitation energy and oscillator strength for the lowest conformer confirm previously reported values.[23]

Furthermore, the first absorption band of **1** can be attributed to the S_0-S_1 transitions that arise mainly from the HOMO to LUMO one-electron excitations. In contrast with **1**, LUMOs of most isomers of **2** do not have significant metal contributions, which is in agreement with previous calculations.[23]

Two-Photon Absorption. TPA for **1** has not been experimentally characterized. TPA calculations for a number of

TABLE 5: TD-mCAMB3LYP/HW-6-31G* Relative Ground (in kilocalories per mole) and OPA Excitation Energy (in electronvolts) and Oscillator Strength (*f*) for 3[a]

isomers	a		b			c			d			e			f			g			h		
state	*E*	*f*	state	*E*	*f*	state	*E*	*f*	state	*E*	*f*	state	*E*	*f*	state	*E*	*f*	state	*E*	*f*	state	*E*	*f*
1^1A_g	0.0		1^1A	0.1		1^1A	0.9		1^1A_g	0.7		$1^1A'$	0.9		1^1A	0.3		1^1A	0.0		$1^1A'$	0.7	
1^1A_u	3.28	3.55	2^1A	3.27	3.47	1^1B	3.17	3.37	1^1B_u	3.04	3.27	$2^1A'$	3.04	3.25	2^1A	3.23	3.47	1^1B	3.28	3.42	$2^1A'$	3.04	3.17
2^1A_g	3.42		3^1A	3.42	0.06	2^1A	3.38	0.07	2^1A_g	3.36		$3^1A'$	3.36	0.00	3^1A	3.41	0.01	2^1A	3.42	0.13	$3^1A'$	3.36	0.12
2^1A_u	3.89	0.00	4^1A	3.84	0.08	3^1A	3.70	0.00	3^1A_g	3.82		$4^1A'$	3.79	0.16	4^1A	3.81	0.08	3^1A	3.89	0.00	$4^1A'$	3.82	0.03
3^1A_g	3.94		5^1A	3.89	0.00	2^1B	3.74	0.24	2^1B_u	3.86	0.35	$1^1A''$	3.84	0.00	5^1A	3.85	0.08	4^1A	3.95	0.01	$5^1A'$	3.87	0.28
3^1A_u	3.96	0.13	6^1A	3.97	0.00	3^1B	4.08	0.08	1^1A_u	3.87	0.00	$5^1A'$	3.88	0.20	6^1A	3.94	0.01	2^1B	3.96	0.12	$1^1A''$	3.87	0.00
4^1A_g	3.98		7^1A	4.01	0.00	4^1A	4.13	0.02	3^1B_u	4.02	0.28	$6^1A'$	4.02	0.30	7^1A	4.03	0.02	3^1B	3.97	0.00	$6^1A'$	4.02	0.28
4^1A_u	4.04	0.00	8^1A	4.05	0.07	4^1B	4.22	0.00	1^1B_g	4.14		$2^1A''$	4.15	0.00	8^1A	4.13	0.09	5^1A	4.04	0.00	$2^1A''$	4.14	0.00
5^1A_u	4.31	0.08	9^1A	4.31	0.07	5^1A	4.30	0.00	4^1B_u	4.31	0.00	$3^1A''$	4.30	0.00	9^1A	4.31	0.00	4^1B	4.31	0.07	$7^1A'$	4.31	0.00
5^1A_g	4.32		10^1A	4.32	0.00				4^1A_g	4.32		$4^1A''$	4.62	0.00	10^1A	4.31	0.05	6^1A	4.32	0.00	$7^1A'$	4.31	0.00
6^1A_u	4.34	0.04	11^1A	4.33	0.02				2^1B_g	4.32		$5^1A''$	4.79	0.00	11^1A	4.33	0.01	5^1B	4.34	0.02	$3^1A''$	4.32	0.00
7^1A_u	4.38	0.16							3^1B_g	4.67								7^1A	4.35	0.01	$4^1A''$	4.68	0.00
6^1A_g	4.35								2^1A_u	4.79	0.00							6^1B	4.38	0.15	$5^1A''$	4.79	0.00

[a] OPA maxima (*f*) measured in benzene for *n*-butyl derivative of **3**: 3.08 eV (shoulder), 3.24 eV ($f = 2.15$), 3.96 eV. [8] INDO/s: 3.16 eV, $f = 3.39$ (trans); 3.17 eV, $f = 3.44$ (cis); TD-B3LYP: 3.00 eV, $f = 2.59$ (trans); 3.01 eV, $f = 2.53$ (cis).[23]

platinum acetylides were previously carried out at the TDHF/6-31G level of theory.[18] TPA was predicted to occur at 5.43 (38 GM), 5.51 (12 GM), and 5.60 eV (18 GM) for the triphosphine derivative of **1** and **2** with PH_3 and $PH_2CH_2PH_2$ ligands, respectively. We found that strong TPA occurs at much lower energies (4.6 to 5.0 eV) for all isomers of **1** (Table 3), which forms a band with a Boltzmann averaged maximum at 4.93 eV and 88 GM (Figure 5). There are several transitions from different conformers that contribute to this band. The lowest **a** conformer, however, does not have the largest contribution. Dominant values come from the **d** and **e** conformers with the phenylene planes that are coplanar with the P−Pt−P axis.

For the tributylphosphine derivative of **2**, Staromlynska et al.[42] measured a TPA coefficient (β) of 0.34 cm/GW in a 0.08 M CH_2Cl_2 solution at 595 nm (4.17 eV) using the z-scan method with 27 ps pulses. This corresponds to a cross-section ($\delta = \beta\hbar\omega/N$, where N is the number density) of 236 GM. Wavelength-dependent measurement by McKay et al.[9] also indicated that TPA occurs in the region 700−560 nm (3.54 to 4.43 eV). However, recent measurements with femtosecond pulses at longer wavelengths produced smaller cross-sections for derivatives of **2**.[6,43] A cross-section of 7 GM at 740 nm (3.35 eV in transition energy) was reported for the unsubstituted tributylphosphine **2** in THF using 180 fs pules.[6,43] Although the small TPA cross-sections were recorded at a much lower energy (near the low-energy edge of the first OPA band; Figures 4 and 6), the high TPA cross-section from a picosecond experiment was therefore speculated to have contributions from excited state absorption. However, previous calculations with INDO/S revealed larger TPA at 3.47 (138 GM) and 4.15 eV (192 GM) for the centrosymmetric **a** conformer.[23] We found that TPA intensities to the first allowed OPA states vanish for centrosymmetric **a** and **d** conformers. They are also small (<1−8 GM) for other conformers (Table 4). This is consistent with the small cross-sections reported at low energies.[6,43] The strong TPA that occurs near 4 eV can be attributed to the first (for **a**−**d**) and second (for **e**−**h**) TPA states. Much stronger TPA is predicted to occur at higher energy. The Boltzmann averaged at 298.15 K gives a peak at 4.57 eV of 771 GM.

B. Chromophores 3, 4, and 5. ***One-Photon Absorption Spectra.*** The ethynyl−benzothiazolylfluorene ligands in **3** (Figure 7) act as electron acceptors, whereas the ethynyl−diphenylaminolfluorene ligands in **4** act as electron donors. We gauged effects of the donor and acceptor by using the phenylethynyl −C≡C−Ph (**1**) and −C≡C−Ph−C≡C−Ph (**2**) as references (Figure 1). Substituting phenylenes with ethynyl−benzothiazolylfluorene groups in **1** and **2** reduces the symmetry of the **a** form of **3** to C_i (Figure 7). This lowest-energy conformer is predicted to have strong S_0-S_1 at 3.28 eV, which is in good

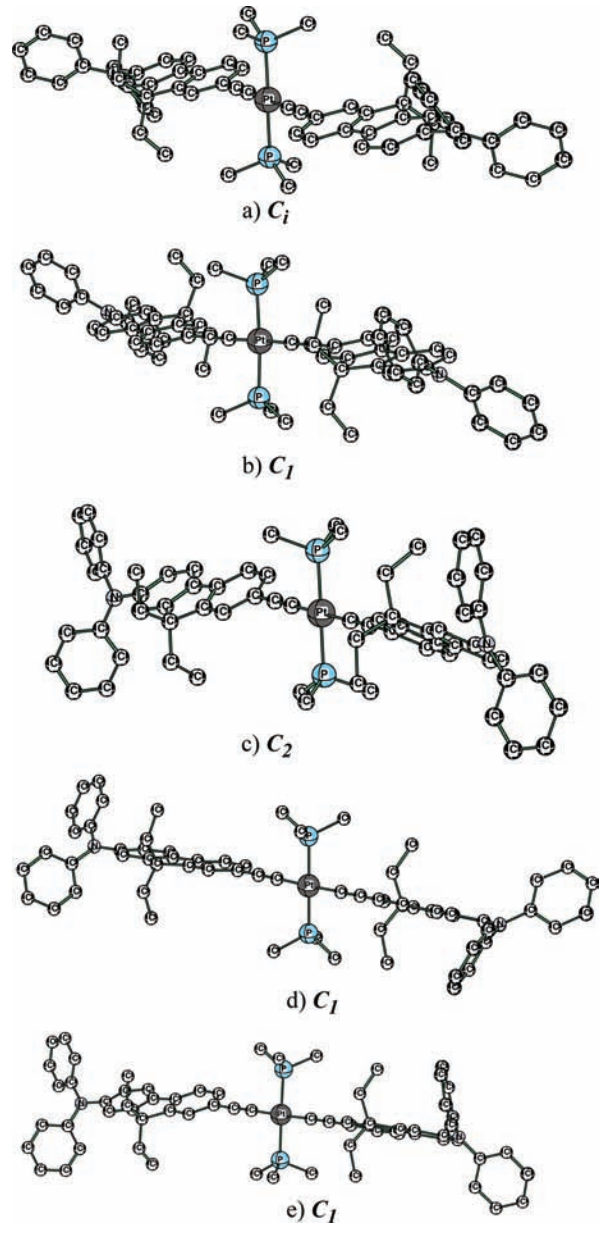

Figure 8. Structural conformers of **4**.

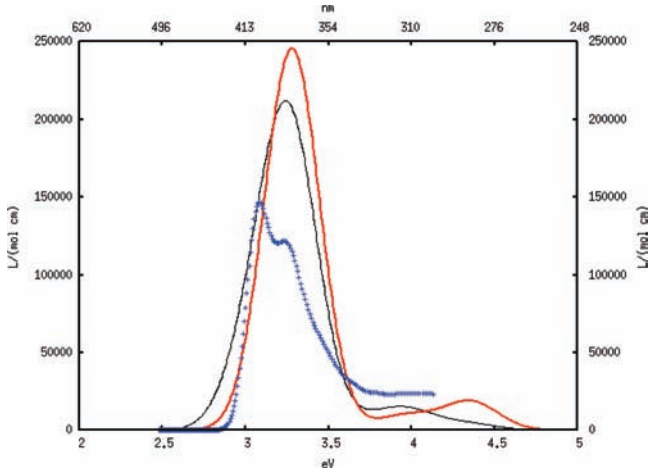

Figure 9. OPA spectra for **3**. Experimental spectrum obtained in benzene at room temperature (+). Computed spectra obtained using fwhm of 0.39 eV for the lowest (**a**) conformer (bold, red) and Boltzmann conformational (**a**−**h**) averaged at 298.15 K (solid).

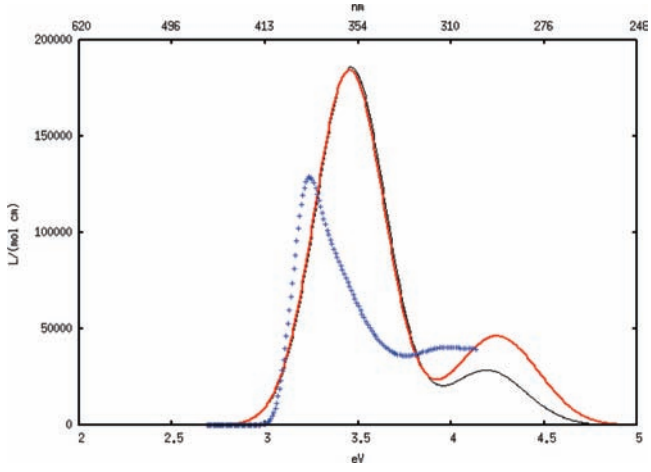

Figure 10. OPA spectra for **4**. Experimental spectrum obtained in benzene at room temperature (+). Computed spectra obtained using fwhm of 0.44 eV for the lowest (**a**) conformer (bold, red) and Boltzmann conformational (**a**−**e**) averaged at 298.15 K (solid).

agreement with the observed OPA maximum at 3.23 eV (Table 5). The oscillator strength of 2.44 obtained by integrating the first band is much smaller than the predicted value. Rotation of the trimethylphosphinyl groups to form the **b** conformer increases the ground-state energy by the same amount (0.1 kcal/mol) found for **1** and **2**. The S_0-S_n transitions are also not significantly affected. Twisting (**c**) and rotating of the benzothiazolylfluorene rings (**d**−**f**) raise the energy by ∼1 kcal/mol. This is significantly greater than the 0.3 kcal/mol found in **1**. The S_0-S_1 transitions of these conformers red-shift by about 0.1 and 0.2 eV because of the twisting and rotating of ethynyl−benzothiazolylfluorene. Note that the **c** and **e** conformers are transition states with small imaginary frequencies of 13*i* (b) and 13*i* cm^{-1} (A″), respectively. The former distorts to a twisted structure with inequivalent Pt−C bonds. For the **e** conformer, the imaginary modes lead to the **b** form. The Boltzmann weighted averaged spectrum at room temperature is shown in Figure 9 along with the experimental spectrum in benzene and the spectrum generated from the lowest-energy conformer. The averaged spectrum has two maxima at 3.25 eV (ε = 2 121 000 M^{-1} cm^{-1}) and 3.94 eV (ε = 155 800 M^{-1} cm^{-1}). The experimental spectrum reveals a lower energy and intensity for the first band. The spectral maximum of the first band is located at 3.08 eV (ε = 1 470 000 M^{-1} cm^{-1}) with a shoulder at ∼3.2 eV.

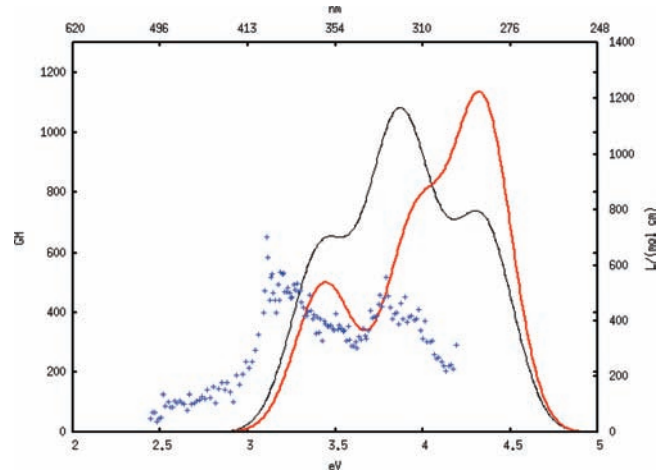

Figure 11. TPA spectra for **3**. Experimental spectrum obtained in benzene at room temperature (+). Computed spectra obtained using fwhm of 0.39 eV for the lowest (**a**) conformer (bold, red) and Boltzmann conformational (**a**−**h**) averaged at 298.15 K (solid).

In **4** (Figure 8), the diphenylamino substituents break the (ethynylfluorene) plane of symmetry. The lowest-energy conformer does have an inversion center with a slightly distorted P−Pt−C angle (87.2°) and tilted (71.8°) fluorenyl rings from 90°. Similar to **1** and **2**, rotation of the trimethylphosphinyl groups is also facile, leading to the **b** conformer, which lies

TABLE 6: TD-mCAMB3LYP/HW-6-31G* Relative Ground (in kilocalories per mole) and OPA Excitation Energy (in electronvolts) and Oscillator Strength (f) for 4 and 5[a]

	4															5					
isomers	**a**			**b**			**c**			**d**			**e**			**a**			**b**		
state	*E*	*f*	state	*E*	*f*	state	*E*	*f*	state	*E*	*f*	state	*E*	*f*	state	*E*	*f*	state	*E*	*f*	state	*E*	*f*
1^1A_g	0.0		1^1A	0.1		1^1A	0.1		1^1A	0.0		1^1A	0.1		1^1A	0.0		1^1A	0.1				
1^1A_u	3.45	3.01	2^1A	3.46	3.01	1^1B	3.44	3.06	2^1A	3.46	2.95	2^1A	3.47	2.99	2^1A	3.30	2.86	2^1A	3.32	2.77			
2^1A_u	3.93	0.02	3^1A	3.61	0.00	2^1A	3.57	0.06	3^1A	3.60	0.09	3^1A	3.59	0.09	3^1A	3.50	0.26	3^1A	3.46	0.05			
3^1A_u	3.99	0.03	4^1A	3.91	0.02	3^1A	3.92	0.00	4^1A	3.93	0.01	4^1A	3.92	0.00	4^1A	3.54	0.26	4^1A	3.54	0.55			
2^1A_u	4.11	0.06	5^1A	3.99	0.01	2^1B	3.93	0.00	5^1A	3.99	0.01	5^1A	3.99	0.01	5^1A	3.94	0.00	5^1A	3.91	0.01			
3^1A_u	4.19	0.45	6^1A	4.00	0.01	3^1B	3.99	0.00	6^1A	3.99	0.01	6^1A	3.99	0.02	6^1A	3.98	0.00	6^1A	3.97	0.00			
4^1A_u	4.23	0.04	7^1A	4.12	0.06	4^1A	3.99	0.02	7^1A	4.11	0.05	7^1A	4.05	0.02	7^1A	3.99	0.01	7^1A	3.99	0.02			
4^1A_u	4.37	0.10	8^1A	4.16	0.00	5^1A	4.19	0.02	8^1A	4.18	0.19	8^1A	4.14	0.02	8^1A	4.06	0.04	8^1A	4.08	0.05			
5^1A_u	4.40	0.20	9^1A	4.19	0.22	4^1B	4.19	0.43	9^1A	4.19	0.25	9^1A	4.19	0.22	9^1A	4.20	0.22	9^1A	4.19	0.22			
			10^1A	4.20	0.24	6^1A	4.19	0.01	10^1A	4.20	0.00	10^1A	4.19	0.23	10^1A	4.26	0.03	10^1A	4.22	0.02			
			11^1A	4.24	0.05	5^1B	4.25	0.23	11^1A	4.21	0.01	11^1A	4.26	0.19	11^1A	4.32	0.03	11^1A	4.32	0.12			

[a] OPA maxima measured in benzene for *n*-butyl derivative of **4**: 3.24 eV (f = 1.7), 3.96 eV.[8] INDO/s: 3.27 eV, f = 2.44 (trans); 3.27 eV, f = 2.39 (cis); TD-B3LYP: 3.26 eV, f = 2.71 (trans); 3.26 eV, f = 2.63 (cis).[23]

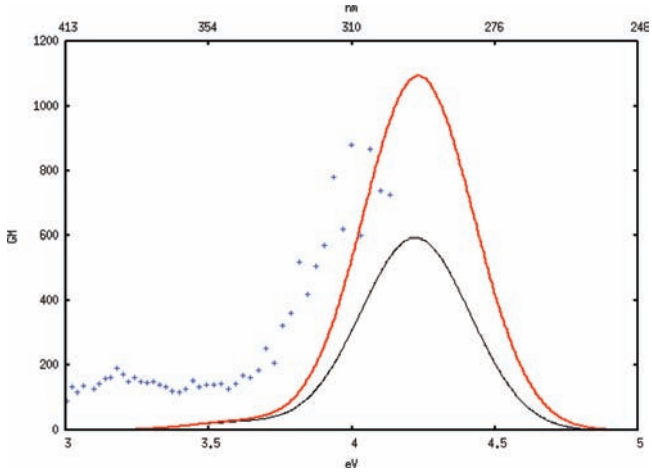

Figure 12. TPA spectra for **4**. Experimental spectrum obtained in benzene at room temperature. Computed spectra obtained using fwhm of 0.44 eV for the lowest (**a**) conformer (bold, red) and Boltzmann conformational (**a**−**e**) averaged at 298.15 K (solid).

only 0.1 kcal/mol (Table 6) higher than the lowest-energy C_i conformer. Interestingly, the twisted C_2 conformer is also a transition state that is slightly higher (0.2 kcal/mol) in energy. This structure with the P−Pt−C angle 87.0° and the (fluorenyl) tilting angle of 60.0° remains twisted after distorting along the 16*i* (*b*) normal modes. Similar to **3**, the predicted spectra of **4** overestimate the experimental energy and intensity (Figure 10). In contrast with other systems, conformational averaging has a small effect on the computed spectrum.

For the donor−acceptor complex **5**, we consider the cis and trans orientations of the methylphosphine groups (Figure 13). The ligands in these conformers are optimized to be gauche with each other. The lowest-energy trans conformer lies 0.1 kcal/mol (Table 6) below the cis structure. The predicted Boltzmann averaged OPA spectrum and the spectrum for lowest conformer (shown in Figure 14) are nearly identical. The energy and extinction coefficient of the first band (3.33 eV, 21 2200 M^{-1} cm^{-1}) is predicted to be similar to corresponding values for **3**. However, the spectral maximum of the second band is predicted to occur at about same energy found at the second peak of **4** but with larger intensity.

Two Photon Absorption. Strong TPA was observed in the excitation region of 600−700 nm, which corresponds to transition energies of 4.13 to 3.54 eV for **3** and **4** (Figures 11 and 12).[8] It was speculated that TPA originates from two-photon allowed states because of the apparent lack of OPA in same energy region. TPA at lower energy is much weaker for **4** (∼150 GM) compared with **3** (∼900 GM). These low-energy transitions occur at or slightly higher energy than the first OPA transitions, where the apparent selection rule violation might be explained either by vibronic coupling or by the existence of at least two conformers, at least one centrosymmetric, whereas the others are not. TPA calculations for different conformers of **3** and **4** indicate that their TPA do have different origins from their OPA counterparts (cf. Tables 5−8). In **3**, the first strong TPA transitions are derived from the second excited states with A_g symmetry for the centrosymmetric conformations (**a** and **d**). However, the third excited states with very small OPA are responsible for strong TPA in the noncentrosymmetric conformations (Table 7). All conformers were also predicted to have large TPA cross-sections near 4 eV. The weighted averaged TPA spectrum exhibits two maxima, with the high-energy band being stronger (Figures 11). The two TPA bands in benzene

TABLE 7: TD-mCAMB3LYP/HW-6-31G* TPA Excitation Energy (in electronvolts) and Cross-Section (*δ*, in GM) using Gaussian Line Shape and Experimental TPA FWHM of 0.39 eV for 3[a]

isomers	**a**		**b**			**c**			**d**			**e**			**f**			**g**			**h**		
state	*E*	*δ*	state	*E*	*δ*	state	*E*	*δ*	state	*E*	*δ*	state	*E*	*δ*	state	*E*	*δ*	state	*E*	*δ*	state	*E*	*δ*
2^1A_g	3.42	494	2^1A	3.27	11	1^1B	3.17	5	2^1A_g	3.36	1013	$2^1A'$	3.04	1	3^1A	3.41	567	1^1B	3.28	11	$2^1A'$	3.04	8
3^1A_g	3.94	606	3^1A	3.42	495	2^1A	3.38	541	3^1A_g	3.82	3505	$3^1A'$	3.36	1043	4^1A	3.81	452	2^1A	3.42	469	$3^1A'$	3.36	965
4^1A_g	3.98	87	4^1A	3.84	282	3^1A	3.70	596	4^1A_g	4.31	25	$4^1A'$	3.79	2560	5^1A	3.85	6	4^1A	3.95	661	$4^1A'$	3.82	3378
5^1A_g	4.32	751	5^1A	3.89	16	2^1B	3.74	1	5^1A_g	4.32	65	$5^1A'$	3.88	579	6^1A	3.94	344	2^1B	3.96	2	$5^1A'$	3.87	6
6^1A_g	4.35	332	6^1A	3.97	10	3^1B	4.08	15				$6^1A'$	4.02	369	7^1A	4.03	42	4^1B	4.31	28	$6^1A'$	4.02	59
						4^1A	4.13	610				$7^1A'$	4.30	5	8^1A	4.13	292	6^1A	4.32	711	$7^1A'$	4.31	13
						4^1B	4.22	4							9^1A	4.31	443	5^1B	4.34	2	$8^1A'$	4.31	25
						5^1A	4.30	2							10^1A	4.31	12	7^1A	4.35	351	10^1A	4.31	12
															11^1A	4.33	6	6^1B	4.38	3	11^1A	4.33	6
																		8^1A	4.40	611			

[a] TPA maxima (cross-sections) measured in benzene for *n*-butyl analog of **3**: ∼3.2 eV (∼500 GM), 3.82 eV (415 GM).[8] Boltzmann factors at 298.15 K for **a**−**g**. Boltzmann averaged maxima: 3.48 eV (660 GM), 4.87 eV (1084 GM). INDO/s: 3.36 eV (172 GM, trans), 3.36 eV (167 GM, cis), 3.87 eV (166 GM, trans), 3.87 eV (159 GM, cis).[23]

TABLE 8: TD-mCAMB3LYP/HW-6-31G* TPA Excitation Energy (*E*, electronvolts)[a,b]

	4															**5**					
isomers	**a**		**b**			**c**			**d**			**e**				**a**			**b**		
state	*E*	*δ*	state	*E*	*δ*	state	*E*	*δ*	state	*E*	*δ*	state	*E*	*δ*		state	*E*	*δ*	state	*E*	*δ*
2^1A_g	3.60	27	3^1A	3.61	25	1^1B	3.44	1	2^1A	3.46	1	2^1A	3.47	1		2^1A	3.30	183	2^1A	3.32	176
3^1A_g	3.99	1	4^1A	3.91	11	2^1A	3.57	28	3^1A	3.61	21	3^1A	3.59	21		3^1A	3.50	5	3^1A	3.46	3
4^1A_g	4.18	722	7^1A	4.12	6	3^1A	3.92	7	4^1A	3.93	5	4^1A	3.92	3		4^1A	3.54	5	4^1A	3.54	6
5^1A_g	4.19	43	8^1A	4.16	454	5^1A	4.19	155	6^1A	3.99	1	6^1A	3.99	1		5^1A	3.94	1	5^1A	3.91	48
6^1A_g	4.29	362	9^1A	4.19	20	4^1B	4.19	2	7^1A	4.11	13	7^1A	4.05	1		6^1A	3.98	87	6^1A	3.97	2
			10^1A	4.20	12	6^1A	4.19	122	8^1A	4.18	14	8^1A	4.14	1		7^1A	3.99	15	8^1A	4.08	115
			11^1A	4.24	228	5^1B	4.25	15	9^1A	4.19	11	9^1A	4.19	14		8^1A	4.06	130	9^1A	4.19	15
									10^1A	4.20	44	10^1A	4.19	13		9^1A	4.20	15			
									11^1A	4.21	565	11^1A	4.26	43							

[a] Cross-sections (*δ*, in GM) are obtained using Gaussian line shape and experimental TPA FWHM of 0.44 and 0.39 eV for **4** and **5**, respectively. [b] TPA maxima (cross-sections) measured in benzene for *n*-butyl analog of **4**: 4.05 eV (780 GM).[8] Boltzmann factors at 298.15 K for **a**−**c**: 0.380, 0.319, 0.301. Boltzmann averaged maxima: 4.22 eV (596 GM). INDO/s: 3.47 eV (34 GM, trans), 3.47 eV (33 GM, cis), 4.11 eV (405 GM, trans), 4.11 eV (386 GM, cis).[23] Boltzmann averaged maxima for **5**: 3.33 eV (185 GM), 4.05 eV (201 GM).

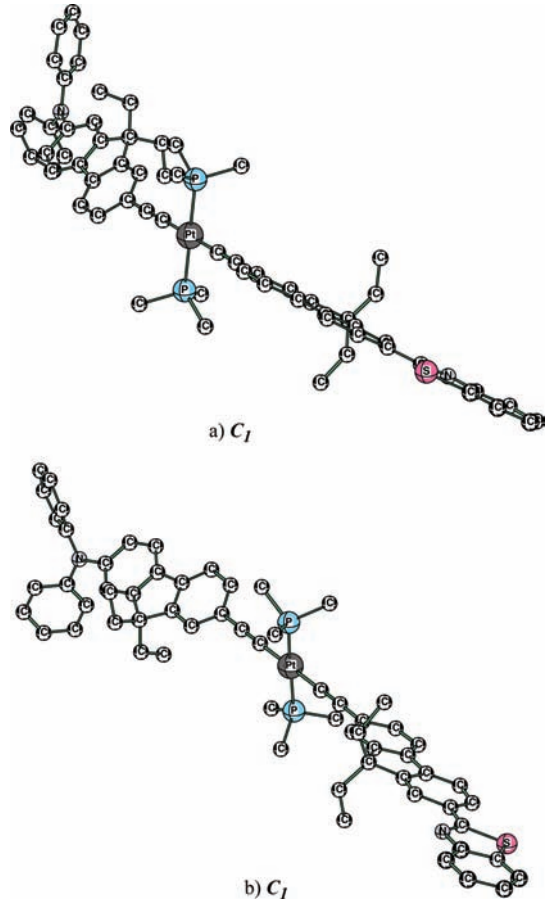

Figure 13. Structural conformers of **5**.

are reported to have similar cross-sections for the *n*-butyl analog of **3**. In **4**, the TPA cross-section of the second excited state (2^1A_g) is quite small for the centrosymmetric **a** conformation (Table 8). TPA cross-sections in this energy region are also small for other conformers. Strong TPA is predicted to occur above 4 eV, which is in agreement with experiment (Figure 12).

The predicted Boltzmann averaged TPA spectrum and the spectrum for the lowest-energy conformer of **5** are shown in Figure 14. The spectra are almost identical at low energy but diverge slightly at high energy. This originates from the first excited state of both conformers with similar TPA cross-sections. For other states, TPA cross-sections for the two conformers deviate significantly (Table 8). The TPA maximum cross-section of 185 GM at 3.33 eV is comparable to the computed values for dipolar fluorene-based chromophores[44] but much smaller than the predicted value for **3** (771 GM at 4.57 eV) and larger than those of **4**. The second TPA band is made up of a number of transitions. The most intense one belongs to the excited states located above 4 eV that underlie the high energy peak at 4.05 with a modest cross-section of 201 GM.

4. Summary and Conclusions

OPA and TPA response calculations have been carried out for a series of platinum acetylides using various basis sets and functionals. The effects of basis sets and functional were found to be small for a trimethylphosphine derivative of **1**. Alkylation induced significant shifts on excitation energies of the unsubstituted chromophore with phosphine ligands for **1**. However, the increase in the chain length (from methyl to *n*-butyl) of phosphine ligands has small effects on the excitation energies and oscillator strengths. All platinum acetylides were found to

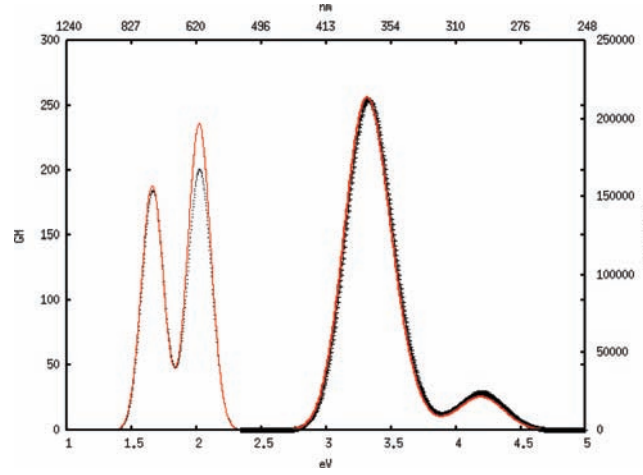

Figure 14. Computed OPA spectra for **5** using fwhm of 0.39 eV for the lowest (**a**) conformer (bold, red) and Boltzmann conformational (**a**, **b**) averaged at 298.15 K (+). Computed TPA spectra for **5** using fwhm of 0.39 eV for the lowest (**a**) conformer (dots) and Boltzmann conformational (**a**, **b**) averaged at 298.15 K (solid).

have multiple low-lying isomers because of the facile rotations of the alkylphosphinyl and phenylene groups. For **1**, the lowest-energy conformer fails to account for the observed S_0-S_n OPA spectrum. Therefore, a Boltzmann weighted average over thermally accessible conformations is important to obtain the final spectra. Conformational effects found for other systems are less pronounced. TPA calculations for **3** and **4** indicate that their TPA do have different origins from their OPA counter parts. This is consistent with the lack of OPA in the same energy region where TPA was experimentally observed. The computed TPA cross-sections at lower energy are found to be smaller for **4** (~30 GM) compared with those for **5** (~190 GM) and **3** (~900 GM), which is in agreement with the observed spectra. Therefore, TPA enhancement for platinum acetylides with two donor or acceptor ligands varies in the order acceptor−acceptor > donor−acceptor > donor−donor.

Acknowledgment. This research has been supported by the Air Force Office of Scientific Research and by CPU time from the Air Force Research Laboratory DoD Supercomputing Resource Center. We gratefully acknowledge a copy of the Dalton program with the CAMB3LYP functional from Prof. Hans Agren and useful discussions with Dr. Joy Haley.

Supporting Information Available: Computed B3LYP excitation energies and oscillator strengths for unsubstituted, *n*-butyl, *n*-propyl, ethyl, and methyl analogs of **1**; conformers of chromophores **2**, **3**, and **4**; and computed excitation energies and oscillator strengths for the methyl analog of **1** using various basis and functional. This material is available free of charge via the Internet at http://pubs.acs.org.

References and Notes

(1) Masai, H.; Sonogashira, K.; Hagihara, N. *Bull. Chem. Soc. Jpn.* **1971**, *44*, 2226–2230.

(2) Wilson, J. S.; Dhoot, A. S.; Seeley, A. J. A. B.; Khan, M. S.; Kohler, A.; Friend, R. H. *Nature* **2001**, *413*, 828–831.

(3) Kohler, A.; Wilson, J. S.; Friend, R. H. *Adv. Mater.* **2002**, *14*, 701–707.

(4) Staromlynska, J.; Chapple, P. B.; Davvy, J. R.; Mckay, T. J. *Proc. SPIE* **1994**, *2229*, 59–66.

(5) Staromlynska, J.; Mckay, T. J.; Wilson, P. *J. Appl. Phys.* **2000**, *88*, 1726.

(6) Vestberg, R.; Westlund, R.; Eriksson, A.; Lopes, C.; Carlsson, M.; Eliasson, B.; Glimsdal, E.; Lindgren, M.; Malmstrøm, E. *Macromolecules* **2006**, *39*, 2238–2246.

(7) Cooper, T. M.; Krein, D. M.; Burke, A. R.; McLean, D. G.; Rogers, J. E.; Slagle, J. E. *J. Phys. Chem. A.* **2006**, *110*, 13370–13378.

(8) Rogers, J. E.; Slagle, J. E.; Krein, D. M.; Burke, A. R.; Hall, B. C.; Fratini, A.; McLean, D. G.; Fleitz, P. A.; Cooper, T. M.; Drobizhev, M.; Makarov, N. S.; Rebane, A.; Kim, K.-Y.; Farley, R.; Schanze, K. S. *Inorg. Chem.* **2007**, *46*, 6483–6494.

(9) McKay, T. J.; Staromlynska, J.; Wilson, P.; Davy, J. *J. Appl. Phys.* **1999**, *85*, 1337–1341.

(10) McKay, T. J.; Staromlynska, J.; Davy, J. R.; Bolger, J. A. *J. Opt. Soc. Am. B* **2001**, *18*, 358–362.

(11) Rogers, J. E.; Cooper, T. M.; Fleitz, P. A.; Glass, D. J.; McLean, D. G. *J. Phys. Chem. A* **2002**, *106*, 10108–10115.

(12) Rogers, J. E.; Hall, B. C.; Hufnagle, D. C.; Slagle, J. E.; Ault, A. P.; McLean, D. G.; Fleitz, P. A.; Cooper, T. M. *J. Chem. Phys.* **2005**, *122*, 214708.

(13) Glimsdal, E.; Dragland, I.; Eliasson, B.; Melo, B.; Lindgren, M. *J. Phys. Chem. A* **2009**, *113*, 3311–3320.

(14) Runge, E.; Gross, E. K. U. *Phys. Rev. Lett.* **1984**, *52*, 997–1000.

(15) Bauernschmitt, R.; Ahlrichs, R. *Chem. Phys. Lett.* **1996**, *256*, 454–464.

(16) Casida, M.; Jamorski, C.; Casida, K. C.; Salahub, D. R. *J. Chem. Phys.* **1998**, *108*, 4439.

(17) Stratmann, R. E.; Scuseria, G. E.; Frisch, M. J. *J. Chem. Phys.* **1998**, *109*, 8218.

(18) Norman, P.; Cronstrand, P.; Ericsson, J. *Chem. Phys.* **2002**, *285*, 207–220.

(19) Emmert, L. A.; Choi, W.; Marshall, J. A.; Yang, Y.; Meyer, L. A.; Brozik, J. A. *J. Phys. Chem. A* **2003**, *107*, 11340–11346.

(20) Batista, E. R.; Martin, R. L. *J. Phys. Chem. A* **2005**, *109*, 9856–9859.

(21) Cooper, T. M.; Blaudeau, J.-P.; Hall, B. C.; Rogers, J. E.; McLean, D. G.; Liu, Y.; Toscano, J. P. *Chem. Phys. Lett.* **2004**, *400*, 239–244.

(22) Minaev, B.; Jansson, E.; Lindgren, M. *J. Chem. Phys.* **2006**, *125*, 094306.

(23) Yang, Z.-D.; Feng, J.-K.; Ren, A.-M. *Inorg. Chem.* **2008**, *47*, 10841–10850.

(24) Kohn, W.; Sham, L. J. *Phys. Rev.* **1965**, *140*, A1133.

(25) Krishnan, R.; Binkley, J. S.; Seeger, R.; Pople, J. A. *J. Chem. Phys.* **1980**, *72*, 650.

(26) Becke, A. D. *J. Chem. Phys.* **1993**, *98*, 5648.

(27) Becke, A. D. *Phys. Rev. A* **1988**, *38*, 3098–3100.

(28) Lee, C.; Yang, W.; Parr, R. G. *Phys. Rev. B* **1988**, *37*, 785–789.

(29) Frisch, M. J.; Trucks, G. W.; Schlegel, H. B.; Scuseria, G. E.; Robb, M. A.; Cheeseman, J. R.; Montgomery, J. A., Jr.; Vreven, T.; Kudin, K. N.; Burant, J. C.; Millam, J. M.; Iyengar, S. S.; Tomasi, J.; Barone, V.; Mennucci, B.; Cossi, M.; Scalmani, G.; Rega, N.; Petersson, G. A.; Nakatsuji, H.; Hada, M.; Ehara, M.; Toyota, K.; Fukuda, R.; Hasegawa, J.; Ishida, M.; Nakajima, T.; Honda, Y.; Kitao, O.; Nakai, H.; Klene, M.; Li, X.; Knox, J. E.; Hratchian, H. P.; Cross, J. B.; Bakken, V.; Adamo, C.; Jaramillo, J.; Gomperts, R.; Stratmann, R. E.; Yazyev, O.; Austin, A. J.; Cammi, R.; Pomelli, C.; Ochterski, J. W.; Ayala, P. Y.; Morokuma, K.; Voth, G. A.; Salvador, P.; Dannenberg, J. J.; Zakrzewski, V. G.; Dapprich, S.; Daniels, A. D.; Strain, M. C.; Farkas, O.; Malick, D. K.; Rabuck, A. D.; Raghavachari, K.; Foresman, J. B.; Ortiz, J. V.; Cui, Q.; Baboul, A. G.; Clifford, S.; Cioslowski, J.; Stefanov, B. B.; Liu, G.; Liashenko, A.; Piskorz, P.; Komaromi, I.; Martin, R. L.; Fox, D. J.; Keith, T.; Al-Laham, M. A.; Peng, C. Y.; Nanayakkara, A.; Challacombe, M.; Gill, P. M. W.; Johnson, B.; Chen, W.; Wong, M. W.; Gonzalez, C.; Pople, J. A. *Gaussian 03*, revision A.11.4; Gaussian, Inc.: Wallingford, CT, 2003.

(30) Yanai, T.; Tew, D. P.; Handy, N. C. *Chem. Phys. Lett.* **2004**, *393*, 51–57.

(31) *Dalton: A Molecular Electronic Structure Program*, release 2.0, 2005. www.kjemi.uio.no/software/dalton.html.

(32) Cossi, M.; Scalmani, G.; Rega, N.; Barone, V. *J. Chem. Phys.* **2002**, *117*, 43.

(33) Cossi, M.; Barone, V. *J. Chem. Phys.* **2001**, *115*, 4708.

(34) Sutherland, R. L. *Handbook of Nonlinear Optics*; Marcel Dekker.: New York, 1996.

(35) Day, P. N.; Nguyen, K. A.; Pachter, R. *J. Phys. Chem. B* **2005**, *109*, 1803–1814.

(36) Goppert-Mayer, M. *Ann. Phys.* **1931**, *9*, 273.

(37) Olsen, J.; Jørgensen, P. *J. Chem. Phys.* **1985**, *82*, 3235.

(38) Salek, P.; Vahtras, O.; Guo, J.; Luo, Y.; Helgaker, T.; Agren, H. *Chem. Phys. Lett.* **2003**, *374*, 446–452.

(39) Day, P. N.; Nguyen, K. A.; Pachter, R. *J. Chem. Phys.* **2006**, *125*, 094103.

(40) Nguyen, K. A.; Day, P. N.; Pachter, R. *J. Chem. Phys.* **2007**, *126*, 094303.

(41) Kondrachova, L.; Paris, K. E.; Sanchez, P. C.; Vega, A. M.; Pyati, R.; Rithner, C. D. *J. Electroanal. Chem.* **2005**, *576*, 287–294.

(42) Staromlynska, J.; McKay, T. J.; Bolger, J. A.; Davy, J. R. *J. Opt. Soc. Am. B* **1998**, *15*, 1731–1736.

(43) Glimsdal, E.; Carlsson, M.; Eliasson, B.; Minaev, B.; Lindgren, M. *J. Phys. Chem. A* **2007**, *111*, 244–250.

(44) Nguyen, K. A.; Day, P. N.; Pachter, R. *Theor. Chem. Acc.* **2008**, *120*, 167–175.

JP905921V